Immobilisation of an anti-platelet adhesion and anti-thrombotic drug (EP224283) on polydopamine coated vascular stent promoting anti-thrombogenic properties

Nicolas Bricout, Feng Chai, Jonathan Sobocinski, Adrien Hertault, William Laure, Alexandre Ung, Patrice Woisel, Joel Lyskawa, Nicolas Blanchemain

Immobilization of an anti-platelet adhesion and anti-thrombotic drug (EP224283) on polydopamine coated vascular stent promoting anti-thrombogenic properties

Nicolas Bricout[1], Feng Chai[1], Jonathan Sobocinski[1], Adrien Hertault[1], William Laure[2], Alexandre Ung[3], Patrice Woisel[2], Joel Lyskawa[2*] and Nicolas Blanchemain[1*]

[1] Univ. Lille, Inserm, CHU Lille, U1008 - Controlled Drug Delivery Systems and Biomaterials, F-59000 Lille, France

[2] Univ. Lille, CNRS, INRA, ENSCL UMR8207, UMET - Unité Matériaux et Transformations, F-59000 Lille, France

[3] Service Hémostase, Regional Hospital Center University of Lille (CHRU-Lille), 2 Avenue Oscar Lambret, 59000 Lille, France

* Corresponding authors: nicolas.blanchemain@univ-lille.fr and joel.lyskawa@univ-lille.fr

Dr. Nicolas Blanchemain
INSERM U1008 - Controlled Drug Delivery Systems and Biomaterials
Univ. Lille, 59006 Lille, France
Tel.: +33 320 626 975

Dr. Joel Lyskawa
UMET – Unité Matériaux Et Transformation – UMR CNRS 8207
Univ. Lille, 59006 Lille, France
Tel.: +33 320 434 751

Key words: Stent, thrombosis, platelet adhesion, dopamine, EP224283, surface functionalization

ABSTRACT

Current vascular drug-eluting stents based on immuno-proliferative drugs would reduce the rate of in-stent restenosis (ISR) but may be associated with a higher risk of acute stent thrombosis due to non-selective activity. In this paper, we aimed to develop a polydopamine (PDA) coated chromium-cobalt (CoCr) stent functionalised with EP224283 (Endotis Pharma SA), which combines both a GPIIbIIIa antagonist (tirofiban moiety) and a factor Xa inhibitor (idraparinux moiety) to reduce acute stent thrombosis.

PDA-coated chromium-cobalt (CoCr) samples were first immersed in a polyethylenimine (PEI, pH 8.5) solution to increase amine function density (36.0±0.1 nmol/cm²) on the CoCr surface. In a second step, avidin was grafted onto CoCr-PDA-PEI through the biotin linkage (strategy 1) or directly by coupling reactions (strategy 2). The HABA titration proved the fixation of biotin onto CoCr-PDA-PEI surface with a density of 0.74 nmol/cm2. The fixation of avidin was demonstrated by water contact angle (WCA) and surface plasmon resonance (SPR). SEM micrograph shows the flexibility of the thin layer coated onto the stent after balloon inflation. Independently of the strategy, a qualitative SEM analysis showed a reduction in platelet activation when the molecule EP224283 was immobilised on avidin. In parallel, the measurement of anticoagulant activity (anti-Xa) revealed a higher anti-factor Xa activity (2.24 IU/mL vs. 0.09 IU/mL in control) when EP224283 was immobilised on avidin. Interestingly, after seven days of degradation, the anticoagulant activity was persistent in both strategies and looked more important with the strategy 2 than in strategy 1.

Throughout this work, we developed an innovative vascular stent through the immobilisation of EP224283 onto CoCr-PDA-PEI-(avidin) system, which provides a promising solution to reduce ISR and thrombosis after stent implantation.

1 Introduction

Endovascular therapies have critically changed the management of both coronary and peripheral artery diseases. The use of bare metal stents (BMS) has improved the results of revascularisation compared to the plain old balloon angioplasty [1] but exposes patients to in-stent restenosis (ISR), thereby increasing the costs of overall treatment. ISR is defined as a ≥ 50% reduction of lumen in the weeks following stent implantation; it could affect up to 30% of patients after a coronary stent and 50% of patients after femoropopliteal interventions [2,3]. Pathophysiological mechanisms of ISR, induced by angioplasty and stent deployment, can be divided into an early and a late phase. The initial endothelial injury caused by the dilatation of the arterial wall and stent implantation promotes platelet aggregation (thrombus formation) and massive local inflammatory response [4]. Gradually, at a later stage, vascular smooth muscle cells (VSMC) present within the arterial wall switch their phenotype influenced by growth factors such as platelet-derived growth factor (PDGF). VSMCs then proliferate and migrate from the media to the intima layers of the arterial wall and increase synthesis of extracellular matrix leading to constrictive arterial remodelling and neointimal hyperplasia [5]. All those late phenomena are continuously triggered by the permanent presence of the metallic stent within the arterial lumen.

The use of drug-eluting stents (DES) has reduced the rate of ISR compared to BMS, but is correlated with a higher risk of late acute stent thrombosis [6]. In this first generation of DESs, late thrombosis was potentially explained by the delayed healing of the arterial wall promoted by the use of a pro-inflammatory and non-absorbable polymers interface that encourages absorption and elution of drug over time and/or by the use of non-selective anti-proliferative drugs (such as paclitaxel and limus derivatives) towards cellular mechanisms of ISR. After DES implantation, long-term dual anti-platelet therapy is required but exposes >10% of patients to major bleeding [7].

Over the recent years, significant efforts have been devoted over the past years to designing new vascular drug delivery platforms limiting inflammation and platelets aggregation phenomena. Those platforms would promote natural vascular healing after device deployment to reduce the risk of ISR, and at the same time would prevent late acute thrombosis. In this context, inspired by the composition of mussel adhesive proteins (MAPs), Lee et al. developed an innovative surface modification method using the dopamine building block that would be applied to vascular platforms [8]. In an alkaline environment, the self-polymerisation of dopamine results in the formation of a robust thin polydopamine (PDA) film, which adheres to almost any type of material. For vascular applications, PDA has emerged as a haemo- and cytocompatible layer promoting endothelial cell (EC) proliferation while reducing that of VSMC [9].

In addition, PDA provides a versatile platform for secondary reactions via Schiff base formation, Michael additions or electrostatic adsorption leading to the grafting of various (bio)molecules or polymers such as selenocystamine, heparin, hyaluronic acid, vascular endothelial growth factor (VEGF), RGD or other peptides on various biomaterials including 316L stainless steel, titanium and CoCr [10–13].

Recently, our group exploited this PDA adhesive layer to enable the grafting of a drug delivery system onto CoCr vascular stent [10–12]. In this work, a cyclodextrin-based polymer grafted onto the stent surface through the PDA layer allowed the loading of different drugs such as paclitaxel and gentamicin [10]. Recently, the innovative molecule EP224283 (Figure 1), which combines a factor Xa-inhibitor (Idraparinux) and a GPIIbIIIa antagonist (Tirofiban) with a biotin recognition site [14], was specially designed by Endotis Pharma SA to address ISR. Very promising preliminary results were obtained showing the beneficial effect of EP224283 on ISR and on stent thrombogenicity after systemic administration in a rat model, which [15] suggests that grafting EP224283 onto the cardiovascular device may possibly

reduce ISR and thrombosis subsequently. Nevertheless, despite latent reactivity of PDA, our efforts to achieve the direct immobilisation of the EP equipped with a biotin function onto polydopamine layer remain unsuccessful.

The present study aims to develop and evaluate two strategies (Figure 2) of immobilisation enabling the grafting of EP224283 on a PDA-coated CoCr vascular stent. In the first strategy, the biotinylation of an amine-rich PDA layer was achieved to immobilise EP224283 on the CoCr platform through the well-known biotin-avidin interactions [16–18]. In the second strategy, avidin was directly immobilised on the amine-rich PDA layer that coats the CoCr platform via coupling reactions and further interacted with EP224283.

2 Materials and methods

2.1 Materials

CoCr disks (thickness 3mm, ⌀14.5 mm, surface 165 mm²) were cut from a cobalt–chromium rod, ISO standards 5832-12 (Co 66.00%, Cr 27.34%, Mo 5.19%, Mn 0.56%, Si 0.39%), Böhler-Edelstahl, Germany). All reagents were purchased from Sigma-Aldrich (St. Louis, MO, USA) and were used as received. Ultrapure water (18.2MΩ, Millipore Milli-Q system, Merck KGaA, Germany) was used for all the experiments. EP224283 (Figure 1) was kindly provided by Endotis Pharma (Romainville, France).

2.2 Methods

2.2.1 Surface functionalisation

Preparation of CoCr samples - CoCr discs were polished with an automatic polishing device (PHOENIX 4000 “Sample Preparation System”, Buehler, Germany) after four cycles of 5min each (using subsequently 600, 1200, 2400 and Supra5 sandpapers, from PRESI, France). Discs were cleaned by a 5-minute ultrasonication (44kHz, Blackstone-NEY Ultrasonics, Jamestown, NY) in acetone, water and ethanol, successively.

The chemical oxidation of CoCr plates was performed using piranha solution, a 70/30 v/v mixture of sulphuric acid (H_2SO_4, 97wt%) and hydrogen peroxide (H_2O_2, 36wt%). Disc samples were immersed in piranha solution for 60 hours at room temperature (RT) under an extractor hood. The discs were then cleaned by ultrasonication in water (30min, 4 times) and dried under nitrogen flow.

Polydopamine (PDA) coating layer - The cleaned CoCr discs were placed in a pillbox containing 5mL of dopamine solution (2mg/mL) in a 10mM Trizma buffer adjusted to pH 8.5 (RT, 400rpm, 16h). The PDA-treated CoCr plates were rinsed with water, dried at 37°C and placed in a clean ventilated oven for a thermal treatment at 150°C for 1 hour [10].

Polyethylenimine (PEI) coating layer - Discs were placed in a pillbox containing 5mL of 50g/L branched PEI (25kDa) solution in a 10mM Trizma buffer adjusted to pH 8.5 (RT, 400rpm, 16h). The PDA-PEI treated CoCr plates were rinsed with water and dried at 37°C.

Avidin immobilisation - Two different strategies for the grafting of avidin were evaluated to promote EP223224 immobilisation (Figure 2).

- **Strategy 1:** PDA-PEI disc samples were placed in a pillbox containing 5mL of D-Biotin (0.4mg/mL, 244g/mol) in a 20mM phosphate buffer saline (PBS) solution adjusted to pH 6, with 1.5molar equivalents of both 1-ethyl-3-(3-dimethylaminopropyl)carbodiimide (EDC) and N-hydroxysuccinimide (NHS) [4°C, 400rpm, 16h]. The PDA-PEI-biotin-treated CoCr discs were rinsed with water and dried at 37°C. Discs were then placed in a 24-well tissue culture polystyrene (TCPS) plate containing 500 µL of avidin solution (1.0mg/mL, 66kDa) in a 10mM PBS solution adjusted to pH 7.4 [RT, 150rpm, 16h]. The PDA-PEI-biotin-avidin treated CoCr discs were rinsed with water and dried at 37°C [19].
- **Strategy 2:** PDA-PEI discs samples were placed in a 24-well TCPS plate containing 500µL of avidin solution (1.0mg/mL) in a 20mM PBS solution adjusted to pH 6 with

1.5molar equivalents of EDC and NHS [4°C, 150rpm, 16 h]. The PDA-PEI-avidin treated CoCr discs were rinsed with water and dried at 37°C.

EP224283 grafting - Discs samples were placed in a 24-well TCPS plate containing 500µL of EP224283 (2.0mg/mL) solution in saline (NaCl 0.9%) [4°C, 1h]. Discs were rinsed twice with 2mL of saline and dried at 37°C under 80rpm for 30min.

The same process of functionalisation was applied on stents ((Multilink 8, Abbott Vascular, Santa Clara, CA., USA) to evaluate the elasticity of the coating after stent expansion at nominal diameter.

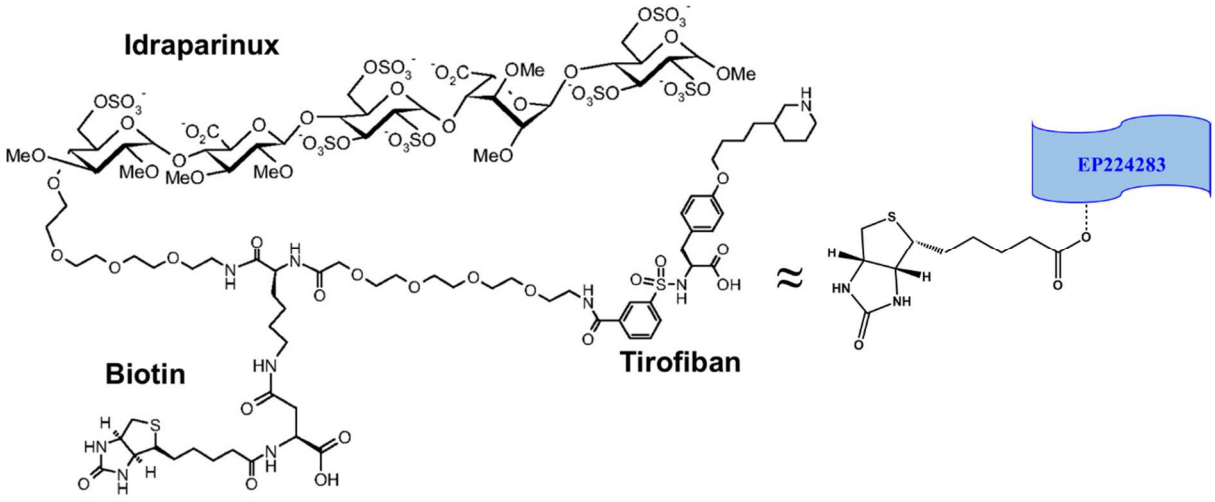

Figure 1: Structure of EP224283 molecule.

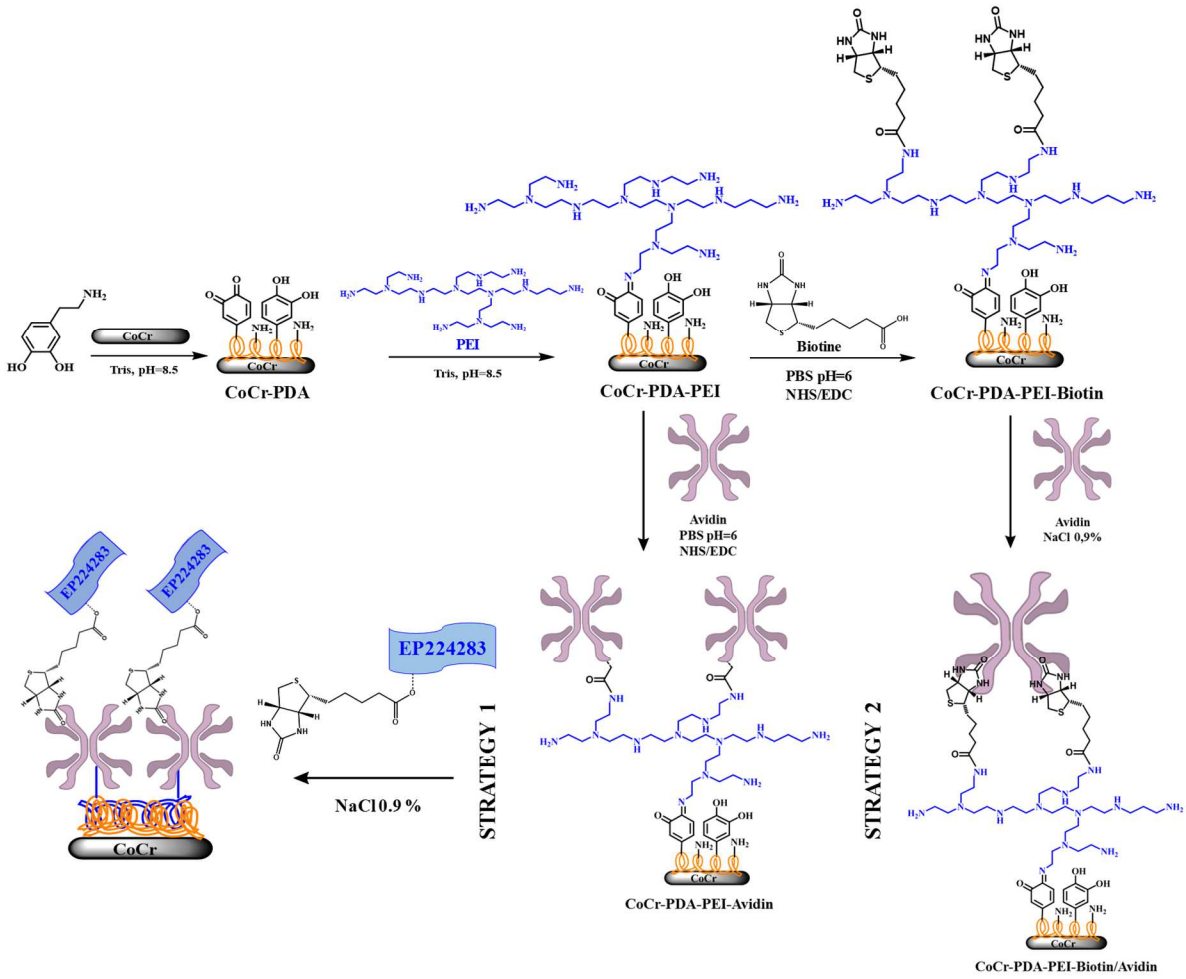

Figure 2: Strategies for CoCr functionalisation and subsequent activation with EP224283. Strategy 1: grafting of avidin onto CoCr-PDA-PEI and subsequent activation with EP224283. Strategy 2: grafting of biotin onto CoCr-PDA-PEI surface, subsequent functionalisation with avidin and activation with EP224283;

2.2.2 Surface characterisation

2.2.2.1 Colorimetric titration with acid orange 2 (AO2)

Colorimetric titration with AO2 was used to determine the number of amino groups immobilised on the PDA-coated surface before and after PEI grafting. Each sample was dipped into 10mL of a $2.5 \cdot 10^{-2}$ mol/L AO2 solution at pH 3 under 60rpm overnight at RT. Samples were then rinsed twice for 5min under stirring in 20 mL of a water solution at pH 3 to eliminate uncomplexed AO2. Desorption was completed by immersing the samples in 1

mL of a water solution at pH 12 overnight at RT under 60rpm. Absorbance was measured at 485nm using UV spectrophotometer (UV-1800, Shimadzu). Results were expressed as AO2 concentration divided by the sample surface area (1.54cm^2).

2.2.2.2 HABA titration

A HABA test was used to determine the amount of biotin function immobilised on the PDA-PEI coated surface before and after biotin grafting. 4-hydroxyazobenzene-2-carboxylic acid (HABA) forms a complex with avidin in solution with absorbance at 500 nm. In the presence of biotin, the HABA/avidin complex dissociates because avidin has a higher affinity constant with biotin (Ka=$10^{-6}M^{-1}$ and $10^{-15}M^{-1}$ for HABA and biotin, respectively). A solution of HABA/avidin ($4.10^{-5}M/10^{-5}M$) was prepared in PBS (pH 7.4). The samples were immersed in 500µl of this solution at 240 rpm (room temperature) and protected from light for an hour. The absorbance of those solutions was then measured at 500nm. The biotin concentration per sample was calculated using the equation below [16–18]:

$$\text{Eq1. [Biotin] (µmol/mL)} = (\text{Abs [HABA/Avidin] } t_0 - \text{Abs [HABA/Avidin] } t_{60min})/ \varepsilon$$

Where ε corresponds to the molar extinction coefficient of the HABA-avidin complex in PBS at 500nm

2.2.2.3 Surface plasmon resonance (SPR)

SPR measurements were recorded using a monochannel AutoLab Springle instrument (Eco Chemie, Netherlands). Polarised laser light (λ=670 nm) is directed to the bottom side of the gold disc (diameter of 2.54 cm) sensor via a hemispheric lens placed on a prism (BK7 having a refractive index of n=1.52), and the reflected light is detected using a photodiode. An autosampler (Eco Chemie, The Netherlands) is used to inject or remove the tested solutions. All SPR measurements were obtained in non-flowing liquid conditions with the circulating pump paused and at RT. The noise level of the SPR angle is about 1 millidegree. After each

addition, the cell was thoroughly washed with PBS (10mM, pH 7.4). All measurements were conducted at 20°C. The substrates were allowed to equilibrate until a steady baseline was observed. The PDA layer was prepared by soaking the Au SPR wafer in a 2 mg/mL dopamine Trizma buffer solution for 1h [20]. After functionalisation, the surface was washed with water and dried under nitrogen flow. PEI Trizma buffer solution (5.0% w/w), avidin (0.1% w/w) or D-Biotin EDC/NHS (0.04% w/w) solution were used for the SPR studies. A biotin functionalised with a fluorescein moiety was used as model molecule mimicking EP224283 for SPR investigations.

2.2.2.4 Scanning electron microscopy (SEM)

Investigations using scanning electron microscopy (SEM) were carried out on a Hitachi S-4700 SEM FEG (field emission gun) operating with an acceleration voltage of 2kV. A thin carbon film was sprayed onto the samples at least 2h before placing them under the beam. A scratch test with a Teflon tip was performed to determine the thickness of the coating layer. To evaluate the elasticity of the coating, balloon-expandable coronary CoCr stents (Multilink 8, Abbott Vascular, Santa Clara, CA., USA) with a nominal diameter from 2.25 mm to 2.75 mm were also functionalized as described in paragraph 2.2.1 to 2.2.5. The stents were inflated (at 8 mmHg up to the nominal diameter) and stent surfaces were then observed through SEM.

2.2.2.5 Wettability

The wettability of discs samples was determined from contact angle measurements. Three separate drops of ultrapure water were positioned on the surface of each disc and numerical images of water drops were acquired using a digital camera [21]. The contact angle was measured with DIGIDROP software (Contact angle meter, GBX scientific instruments, France).

2.2.3 In vitro biological evaluation

2.2.3.1 Cell vitality and cell proliferation assay.

All samples were sterilised in ethanol (96%) for 1min. Cell culture was performed according to ISO 10993-5/EN 30993-5 with a human umbilical vascular endothelial cell line (HUVEC, C12200, Promocell GmbH, Heidelberg, Germany). HUVEC were cultured in Endothelial Cell Growth Medium MV (Promocell GmbH, Heidelberg, Germany) enriched with Endothelial Cell Growth Supplement Mix (Promocell GmbH, Heidelberg, Germany), streptomycin (0.1g/L) and penicillin (100IU/mL), at 37°C in a CO_2 incubator (BINDER C170, Tuttlingen, Germany) with 5% CO_2/95% atmosphere and 100% of relative humidity.

Disc samples were placed at the bottom of 24-wells cell culture plates (COSTAR®, Starlab, Orsay, France) and 10.000 cells in 1mL of culture medium were added in each well. Wells without a sample disc (*i.e.* TCPS) were used as the control. The proliferation and vitality of cells were then evaluated after 1 and 3 days.

Cell vitality was assessed using the non-toxic alamarBlue dye (UptiBlue™, Interchim). The culture medium was removed, and 500µL of diluted blue dye (10% volume of culture medium) were added to each sample. After incubation at 37°C for 3h, 150µL of this solution were transferred to a 96-well plate (Fluoro-LumiNunc™, ThermoScientific, France) and the fluorescence intensity was measured with a Twinkle LB970TM fluorometer (Berthold, France) at an excitation wavelength of 530nm and at an emission wavelength of 590nm [22]. Cell vitality is expressed as a percentage of the control (TCPS).

Cell proliferation was further assessed using trypsin (0.3mL) to detach the adherent cells after alamarBlue cell vitality assay. Cell counting was performed using a Coulter ZI cell counter (Beckman Coulter, Danaher, Germany). Cell proliferation was expressed as a percentage of the control (TCPS). All data are expressed as the mean percentage ± SD of three separate experiments.

2.2.3.2 Anticoagulation activity

The evaluation of the coagulation cascade was carried out in order to determine the antiXa activity of grafted EP224283 on CoCr samples. CoCr, CoCr-PDA-PEI-avidin and CoCr-PDA-PEI-biotin-avidin discs were placed in a 24-well TCPS plate (three discs per group). A 2mg/ml EP224283 solution was prepared with isotonic saline, 500µL of which were deposited in each well for 1h at 4°C. Afterwards, samples were rinsed twice with 2mL of isotonic saline and dried for 30min at 37°C under 80rpm. Human whole blood was freshly collected from healthy volunteers in sodium citrate (0.109M) Vacutainer® blood collection tube (BD, Le Pont-de-Claix CEDEX, France), and 800µL whole blood was then added to each well and incubated at 37°C for 30min under 80 rpm. As the control, TCPS and EP224283-coated TCPS were also evaluated. The blood was withdrawn from the sample and centrifuged (Centrifuge 5415 R, Eppendorf AG, Germany) for 15min at 2500g at 14°C to obtain the platelet-poor plasma (PPP). The PPP was analysed with medical coagulation analyser (STAGO STA R Max2) to determine anti-FXa activity (UI/ml), expressed as the mean ± SD of three separate experiments with respect to the control (TCPS).

2.2.3.3 Platelet adhesion assay: quantification and morphology

Human blood was sampled as previously described. Platelet-rich plasma (PRP) was prepared by centrifuging (Allegra X12-R centrifuge, Beckman Coulter, Fullerton, CA) the blood (300g, 5min, 25°C). 100µL of fresh PRP was added onto each disc and incubated for 45min at 37°C. Non-adherent platelets were then removed by gently rinsing the sample twice with an isotonic saline. The quantification of adhered platelet was determined by measuring lactate dehydrogenase (LDH) activity with an LDH kit (Roche life sciences, Meylan CEDEX, France) according to the manufacturer's recommendations. The morphology of the adherent platelets was studied, after fixing with 2.5% glutaraldehyde solution, gradient dehydration in

50, 75, 90, 100% ethanol solutions and carbon sputtering, by scanning electron microscopy (SEM, Hitachi S-4700 SEM FEG).

2.2.4 Degradation study

Functionalised CoCr disc samples from two strategies were immersed in 5mL of PBS (10mM, pH 7.4) under 80rpm at 37°C. EP224283-coated bare CoCr discs were also tested as the control. Anti-FXa activity assays were performed, as previously described, on the disc sample withdrawn from PBS at different time intervals (0, 1, 3 and 7 days) to evaluate the degradation of the EP224283 coating layer (represented by the absence of anti-FXa activity).

2.2.5 Statistical analysis

Quantitative variables were expressed as mean with standard deviation (SD). The comparison of two independent groups were performed with a Student *t*-test if normality was met and otherwise with a Mann-Whitney test. Comparison of more than two groups were performed with a non-parametric Kolmogorov-Smirnov test. A $p<0.05$ value was considered as significant. All statistical analyses were performed with the SPSS software (IBM Corp. Released 2011. IBM SPSS Statistics for Windows, version 20.0. Armonk, NY: IBM Corp.).

3 Results and discussion

With the objective of grafting the biotin moiety (integrating a carboxylic acid function) onto the CoCr surface for the subsequent immobilisation of EP224283 through biotin/avidin interactions, we used an amine rich polydopamine layer for the functionalisation. Interestingly, Yang et al. [12] recently reported a mussel-inspired one-step procedure allowing the covalent immobilisation of heparin on an amine-rich polydopamine coating. This adhesive layer was obtained by in situ co-polymerisation of dopamine and polyethyleneimine (PEI) onto a 316L stainless steel surface and provides an amine density of 26 nmol/cm^2 while the polydopamine layer alone shows an amine density of no more than 4 nmol/cm^2. In their work,

the amine groups at the metallic surface (316LSS) were the cornerstone of the functionalisation process to obtain heparin grafting through EDC coupling reactions. In this work, a different strategy was used to generate the amine-rich PDA layer consisting in the post-functionalisation of PDA layer with PEI via Michael additions and Schiff base reaction increasing the density of amine functions available at surface for coupling reactions.

3.1 Quantitative evaluation of amine functions grafted onto CoCr surfaces

The number of amine functions grafted onto CoCr, CoCr-PDA, CoCr-PDA-biotin, CoCr-PDA-PEI and CoCr-PDA-PEI-biotin surfaces was quantified by colorimetric titration with AOII. As depicted in Figure 3, no amine function was detected on the bare CoCr surface while a density of 10.4±0.9nmol/cm² of amine functions was measured on the CoCr-PDA surface. These results are in accordance with previous work dealing with the functionalisation of CoCr surfaces by PDA [10] and were attributed to the free catecholamine fragments incorporated in the PDA structure. In the same way, no difference was observed between CoCr-PDA and CoCr-PDA-biotin, suggesting that the direct grafting of biotin onto the PDA layer did not occur. Interestingly, the CoCr-PDA samples functionalised with PEI exhibited a higher density of amine functions compared to the CoCr-PDA surfaces (36.0±0.1nmol/cm² vs. 10.4±0.9nmol/cm², $p<0.001$). These results show a higher density of amino groups grafted onto the surface compared to the method recently proposed by Liu et al. [23], which consists of the generation of an amine-rich dopamine layer through a one-step catechol/PEI copolymer coating (15.1±2.7 nmol/cm²) and are similar to those observed by Weng et al. [11].

Then, after coupling reactions with biotin, a significant decrease in the density of amine functions was observed (25.5±2.2 nmol/cm², $p<0.015$) at the surface, demonstrating the covalent grafting of the biotin ligand onto the CoCr-PDA-PEI surface. In this way, a biotin grafting density of 10.4±1nmol/cm², ($p<0.001$) could be estimated with regard to the decrease of amine density at the surface.

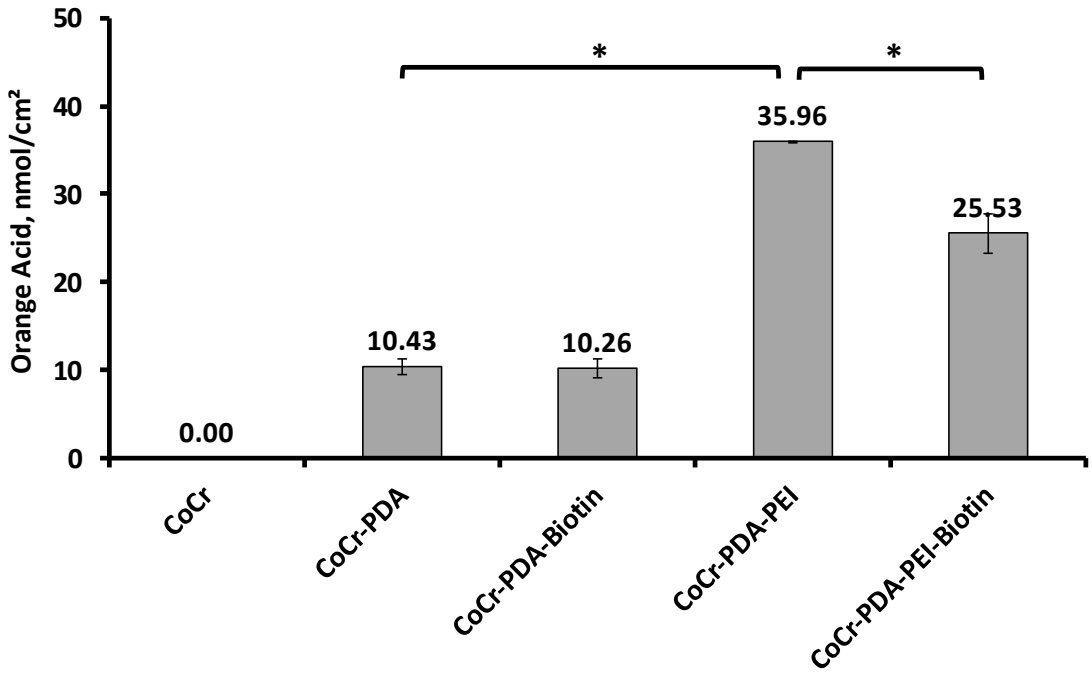

*Figure 3: Acid orange 2 colorimetric titrations of amino functions grafted onto CoCr, CoCr-PDA, CoCr-PDA-PEI and CoCr-PDA-PEI-biotin surfaces. (mean±SD, n=3; * p<0.001).*

3.2 Evaluation of biotin and avidin grafting onto CoCr modified surfaces

The ability of avidin to be grafted onto CoCr surfaces was investigated by HABA-avidin test and surface plasmon resonance. The HABA-avidin test was first used as quantitative method to evaluate the amount of biotin available on the CoCr-PDA and CoCr-PDA-PEI surfaces after NHS/EDC coupling reactions with biotin.

As depicted in Figure 4, HABA-avidin tests show the interactions between avidin and the biotin-functionalised CoCr surfaces. Indeed, biotin densities as high as 0.55 nmol/cm^2 and 0.74 nmol/cm^2 were observed on CoCr-PDA and CoCr-PDA-PEI functionalised samples respectively thus demonstrating the grafting of the biotin moiety. It is worth noting that no significant interactions were observed between avidin and PDA or PDA-PEI surfaces thus highlighting the key role played by the biotin unit.

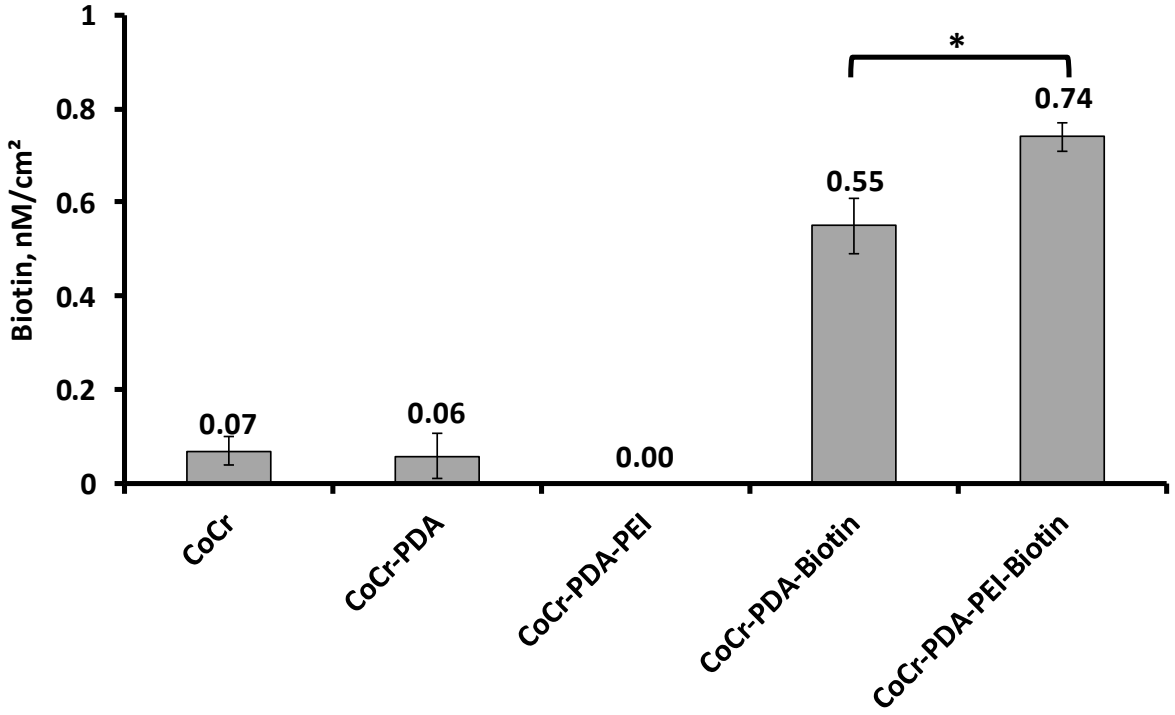

Figure 4: HABA-avidin titrations of the biotin moiety grafted onto CoCr, CoCr-PDA, CoCr-PDA-PEI and CoCr-PDA-PEI-biotin surfaces. (mean±SD, n = 3; * $p<0.001$).

Surface plasmon resonance (SPR) was then used as a non-invasive optical method to monitor, in real time, the binding events on the CoCr functionalised surfaces according to the change of the refractive index in the close vicinity of the metal layer [20]. In this work, SPR was used to investigate (i) the formation and importance of the PDA-PEI layer (ii) the immobilisation of avidin onto CoCr-PDA-PEI-biotin and CoCr-PDA-PEI surfaces and iii) the fixation of a functionalised biotin as a model molecule mimicking EP224283 onto CoCr-PDA-PEI-biotin-avidin and CoCr-PDA-PEI-avidin surfaces.

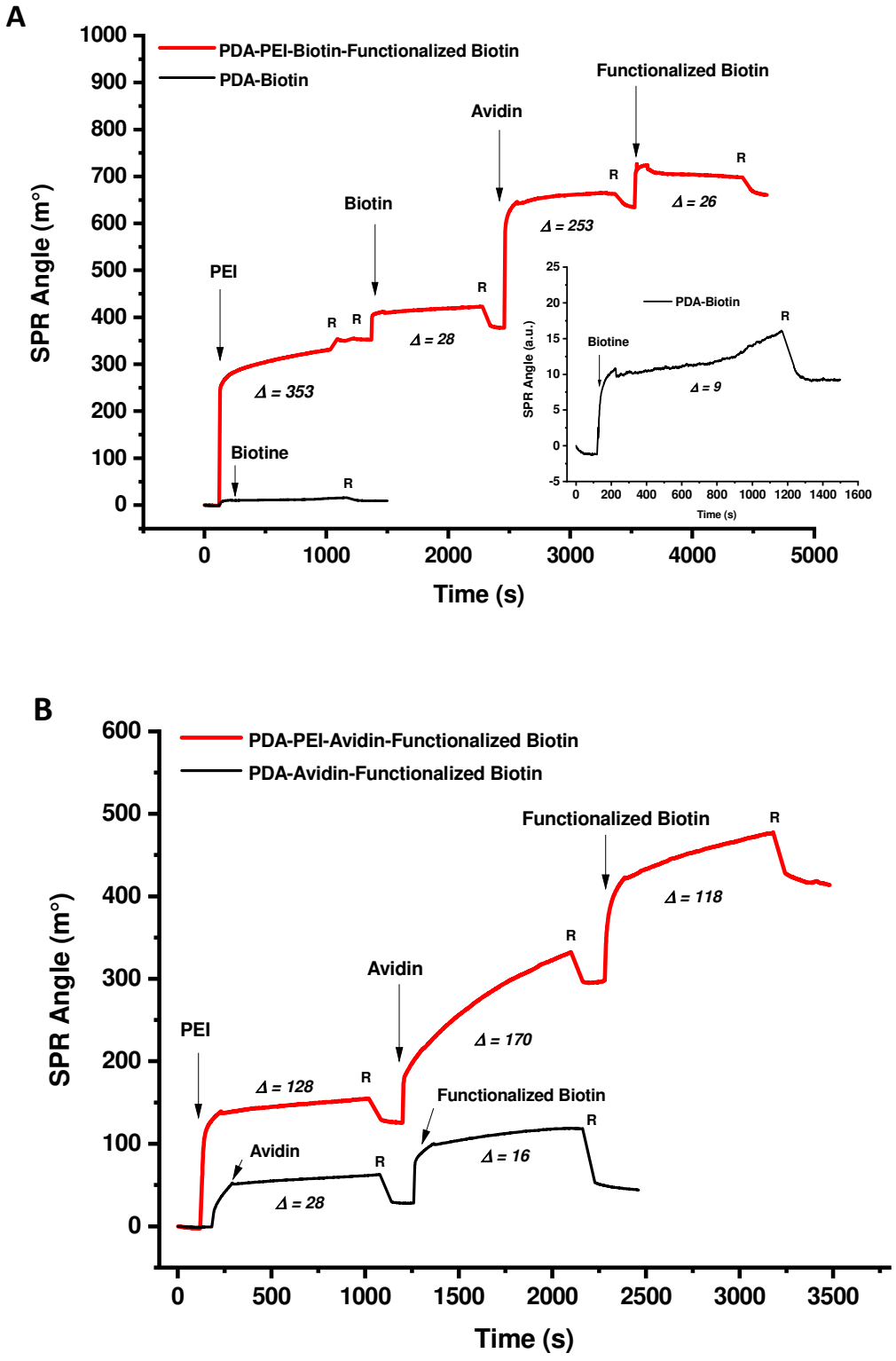

Figure 5: SPR sensogram recorded on a polydopamine coated gold surface during the subsequent injections of PEI, biotin-NHS; avidin and functionalised biotin (a) and PEI, avidin-NHS and functionalised biotin (b).

Firstly, activated biotin-NHS and avidin-NHS were directly injected onto CoCr-PDA surfaces. As depicted in Figures 5a and 5b, very slight shifts in the resonance angles (Θ) (28 m° and 9 m° for biotin and avidin respectively) were observed, indicating that very little materials was immobilised on the PDA layer of the CoCr surface. As a consequence, an intermediate PEI layer was added to increase the density of amine functions with the objective of improving the grafting efficiency (Fig. 3). For this purpose, an aqueous PEI Trizma buffer solution (5.0%w/w) at pH 8.4 was injected onto an SPR gold wafer functionalised with PDA (Figure 5a and 5b). After flushing the wafer with the PBS buffer solution (0.1M, pH 7.4), a shift in the resonance angle (Θ) was clearly observed (Δ=128-353m°), indicating the immobilisation of the PEI layer onto the PDA-coated gold surface. It is worth noting that no change in the SPR angle was observed after injections of PEI Trizma buffer solution onto the unmodified gold wafer demonstrating the key role played by the catechol/quinone groups of PDA in the grafting of PEI. As depicted in Figure 5a, upon the injection of an aqueous solution of *in situ* generated biotin-NHS (0.04%w/w) onto the CoCr-PDA-PEI surface and subsequent rinsing with PBS buffer, a slight increase of the resonance angle (Θ) was highlighted (Δ=28m°) corroborating the grafting of biotin onto the Au-PDA-PEI surface. This moderate change in the SPR angle is likely due to the smaller molecular weight of the biotin ligand compared to PEI and avidin. As expected, upon the injection of an aqueous solution of avidin (Figure 5a) onto the CoCr-PDA-PEI-biotin surface, an increase of the SPR angle (Δ=253m°) was observed indicating the immobilization of the avidin onto the biotinylated layer. Nevertheless, the subsequent injection of the functionalised biotin mimicking EP224283 onto the avidin layer leads to very small changes in the SPR angle suggesting that the complexation sites of avidin are nearly saturated in this case. Interestingly, the injection of in situ generated avidin-NHS (Figure 5b) onto CoCr-PDA-PEI surfaces leads to the immobilisation of a significant amount of avidin according to the increase observed with the

SPR angle (Δ=170m°). However, the visual inspection of the shape of the SPR binding profile reflects a weaker slope in the coupling reaction with PEI and avidin-NHS compared to biotin-avidin interactions. These results are attributed to the high affinity of avidin for biotin (K_{ass}~$10^{15}M^{-1}$), which leads to fast surface functionalisation while the coupling reaction between PEI and avidin-NHS occurs with lower kinetics and consequently requires more time for surface functionalisation [24]. Finally, a significant shift of the SPR angle (Δ=118m°) was observed after injection of the functionalised biotin onto the avidin surface, thus demonstrating that the avidin binding site is available for biotin binding in this context.

3.3 Contact-angle measurement

The impact of the functionalisation processes on the wettability of CoCr surfaces was studied with static water contact angle measurements. As depicted in Figure 6, the CoCr surface exhibits a contact angle of 75±1° [25]. This surface became more hydrophilic after modification with PDA (67±2°, $p<0.001$) in accordance with the grafting of both catechol and quinone groups onto the CoCr surface [23]. This value decreases to 56±2° ($p<0.001$) after subsequent functionalisation with PEI due to the presence of hydrophilic amine groups on the CoCr surface. No significant change was observed after grafting of biotin onto the CoCr-PDA-PEI surface likely due to the small amount of deposited biotin compared to polymers and its hydrophilic character. The grafting of avidin was confirmed in both cases as a significant decrease of the contact angle to 43.5±6.2° ($p<0.001$) for CoCr-PDA-PEI-avidin and 31.0±3.4° ($p<0.001$) for CoCr-PDA-PEI-biotin-avidin was observed. These results are close to those measured by Chen et al. [26] during the immobilisation of avidin onto a PDA-modified titanium surface thus further corroborating the effective grafting of avidin onto CoCr surfaces, through those two strategies.

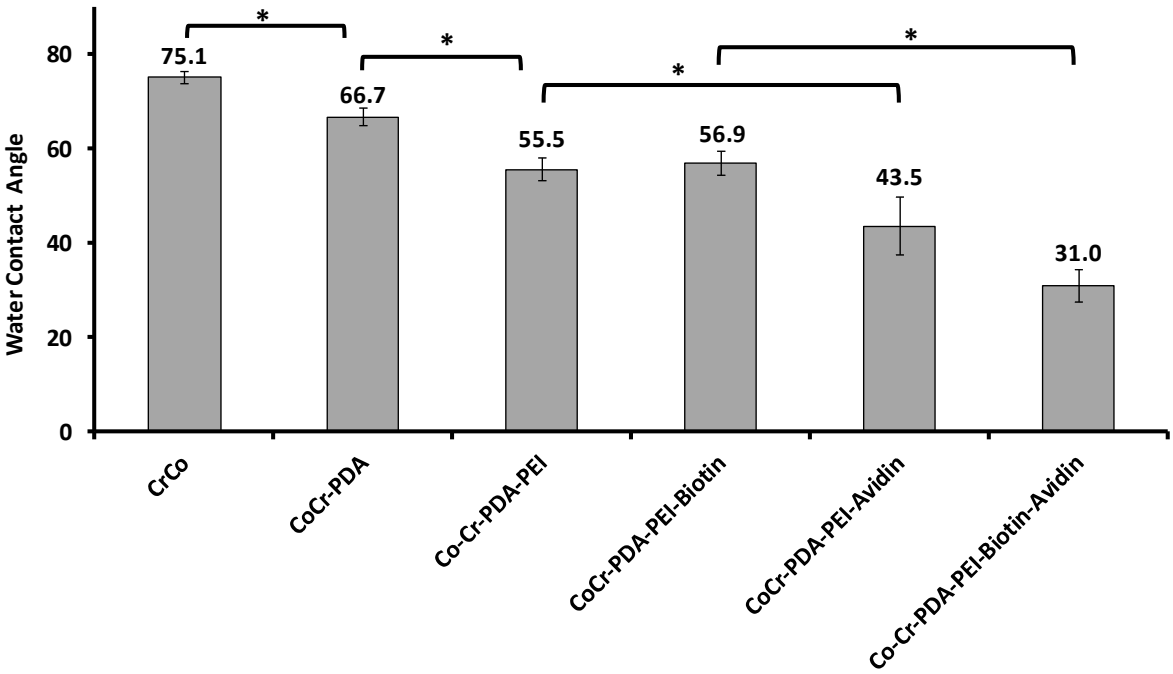

Figure 6: Evolution of water Contact Angle measurements throughout the functionalisation processes (* $p<0.001$).

3.4 Coating morphologies

The morphologies of the different layers were observed by scanning electron microscopy (SEM). SEM images of the CoCr-PDA sample confirming the presence of the PDA-coated layer on the CoCr surface (Figure 7a) as a dense and almost homogeneous film were observed. Small particles were depicted within the PDA layer that were attributed to the formation of melanin-like nanoparticles during the polymerisation of PDA [27]. The PDA film thickness was estimated up to 50nm from SEM images after scratching the coated surface with a Teflon tip. These results are in accordance with our previous results dealing with the functionalisation of polydopamine-based surfaces [10]. No significant change in the morphology and film thickness was observed on SEM images after PEI, biotin or avidin grafting. These observations are in agreement with Chen et al.'s work related to the immobilisation of serum albumin on an avidin-modified PDA layer and could be explained by

the 1000-time lower mass of PEI, avidin (~400ng/cm², [26]) and biotin compared to PDA itself (~600 µg/cm², [20]).

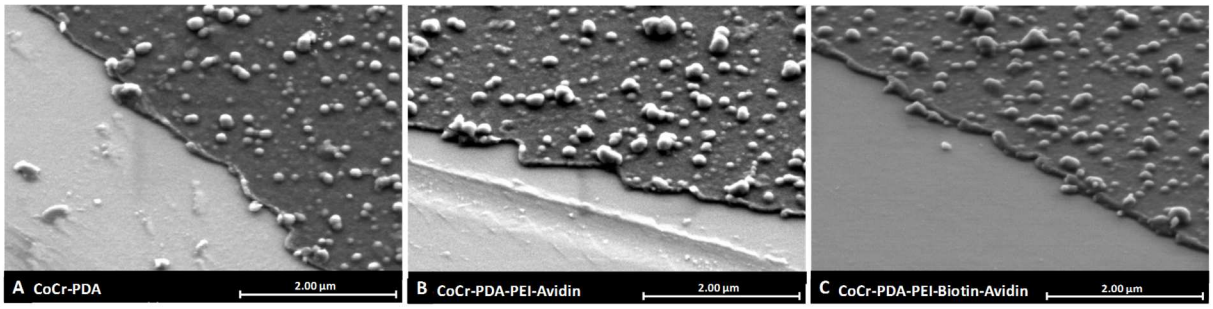

Figure 7: SEM images of CoCr-PDA (A), CoCr-PDA-PEI-avidin (B) and CoCr-PDA-PEI-biotin-avidin (C) surfaces.

Finally, both functionalisation processes were applied to a balloon-expandable CoCr coronary stent (Multi-LinkVision, AbbottVascular, Inc., Santa Clara, CA). SEM analyses were performed to evaluate the morphology of the coated stents (Figure 8) as well as the stability of the coating after balloon inflation at nominal diameter (8bars). As depicted in Figure 8, a dense and homogeneous polymer layer can be observed on the stent surface in both cases. Interestingly, the coating layer completely covered the stent and visual inspection of the coated device by SEM did not reveal the presence of cracks or defects even after balloon inflation. In conclusion, these investigations demonstrated the applicability and feasibility of the functionalisation process in the context of medical applications, in particular in the treatment of ISR.

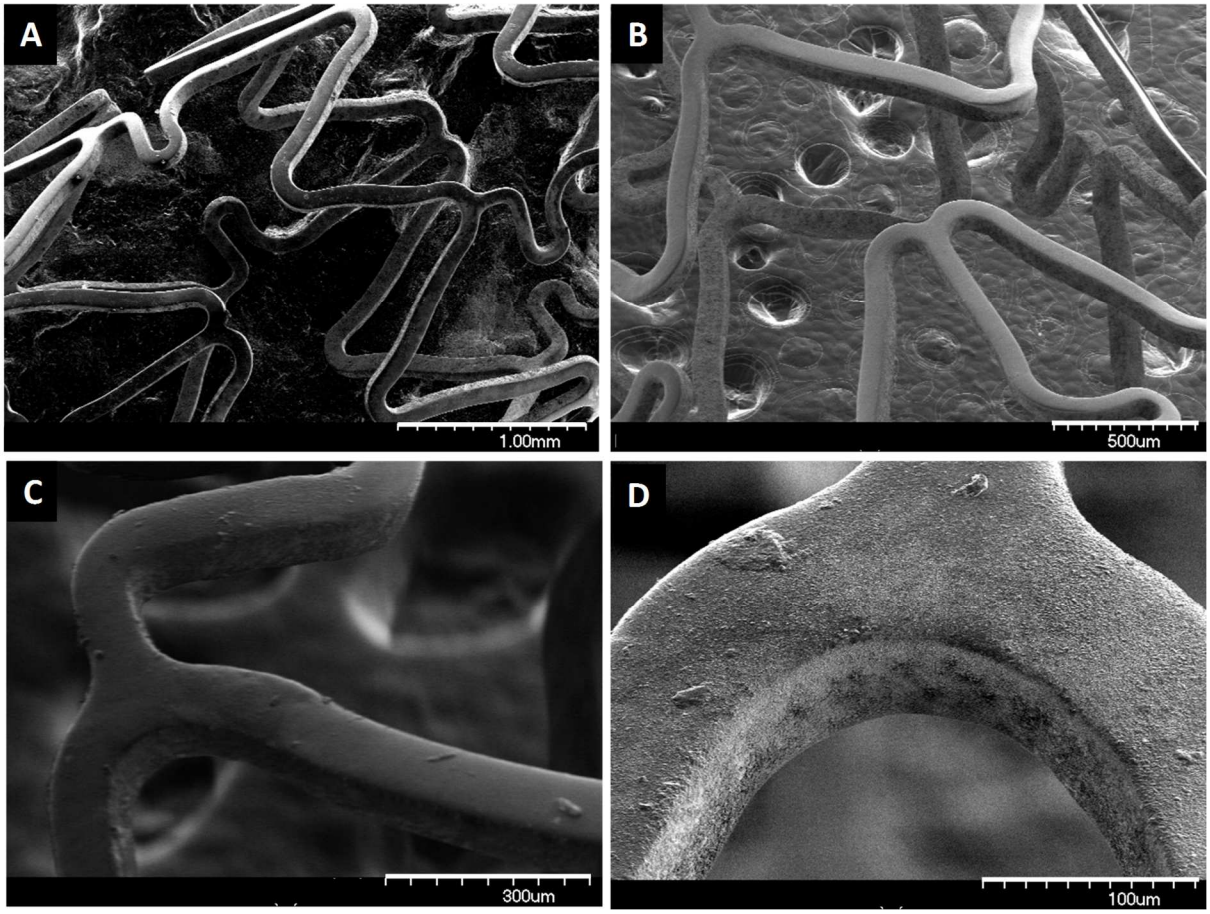

Figure 8: SEM images of PDA-PEI-avidin (A, D) and PDA-PEI-biotin-avidin (B, C) functionalised CoCr stents after balloon inflation.

3.5 Cytocompatibility

Biological evaluations of bare and functionalised CoCr samples were performed with primary human endothelial cells (HUVEC) by direct contact method. Cell vitality and proliferation were assessed using alamarBlue assay and counting numbers of living cells on the sample. As depicted in Figure 9, bare CoCr surfaces exhibited good cell vitality and proliferation of HUVEC after 1 day (80±7%) and 3 days (60±5%) of culture. Compared to bare CoCr, the PDA-PEI grafted discs induced a decrease of both proliferation and vitality of HUVEC after 1 day (60±7%) and 3 days (30±6%). Otherwise, on the basis of CoCr-PDA-PEI, no additional impact on HUVEC was induced after the grafting of avidin and EP224283. Indeed, we

already proved the non-toxicity of EP224283 on HUVEC [19]. It is worth noting that PDA coating has proved to have good surface wettability, bioactivity and excellent interactions [28–31] with various cell types involved in different biomedical applications including various cell adhesion [32,33] bone regeneration, blood compatibility and antimicrobial activity. However, as already reported by our group[10], cytotoxic effects would have been also reported in other studies. Thus, Li et al. [34] thus observed a decrease of HUVEC proliferation on a PDA/PEI copolymer-modified surface, which was interpreted by the potential toxicity of the PDA/PEI layer itself and the higher number of amine functions exposed at the surface of the platform. Elsewhere, Graham et al. [35] explained the cytotoxicity of PDA through the presence of free dopamine fragments (and free-catechol functions) entrapped within the PDA film. Ding et al. [36] further proposed an explanation including a two-step mechanism of formation of PDA layer: a primary building block of (DHI)2/PCA trimer complex is firstly obtained by covalent interactions in the initial stage of polymerisation, and cytotoxic (DHI)2/PCA trimer particles linked through non-covalent interactions to PDA are generated in the latter stage.

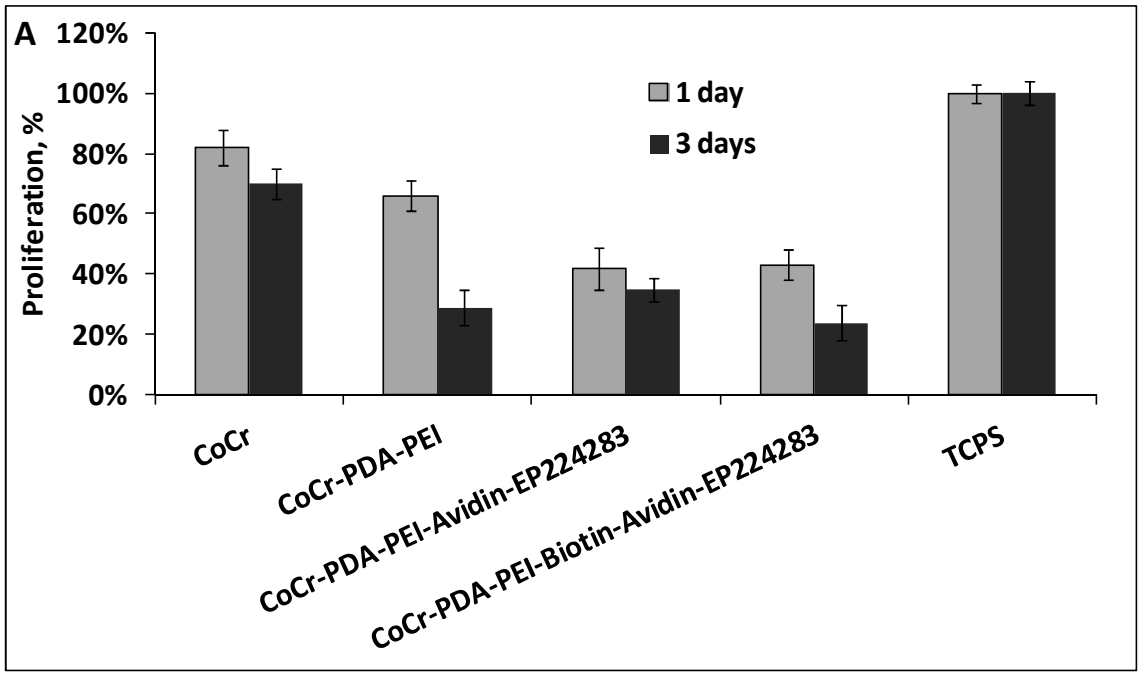

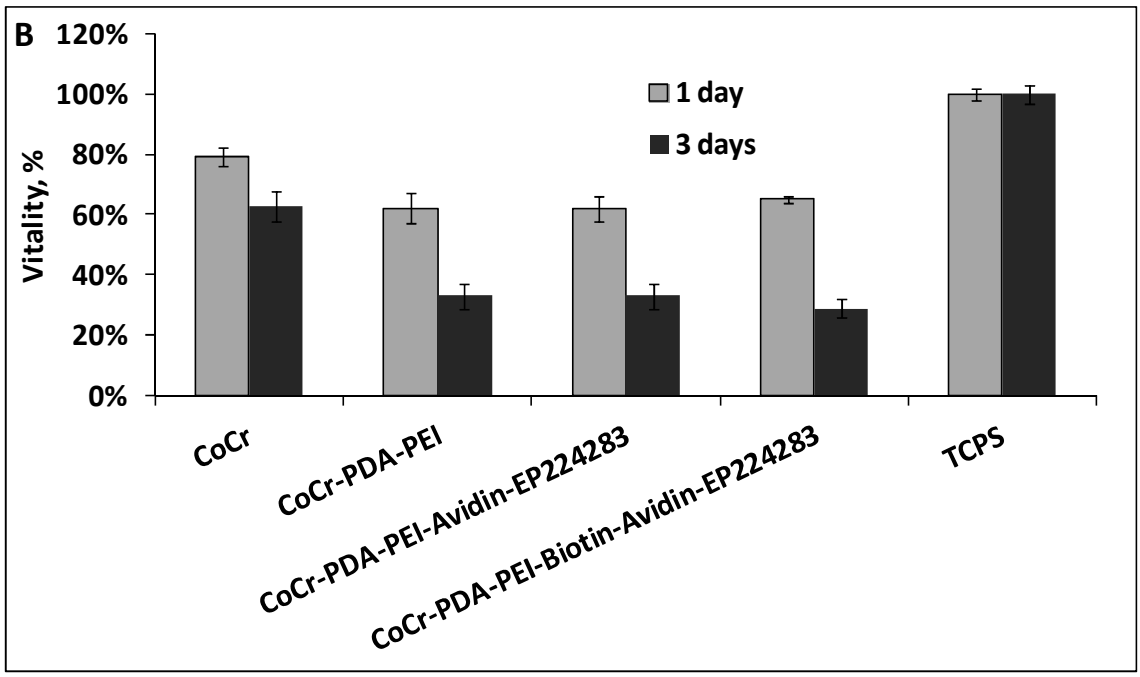

Figure 9: Proliferation and vitality rate by cell counting method (A) and vitality by alamarBlue assay (B) of HUVEC on bare and functionalised CoCr samples after 1 and 3 days of culture (37°C, 5% CO_2, 100% relative humidity), without culture medium renewal.

3.6 Anticoagulation activity: anti-FXa assay

The molecule EP224283 was synthetised to provide both anti-FXa/anti-thrombin generation (idraparinux) and anti-platelet aggregation (tirofiban) activities. A previous study [15] by our group demonstrated in a rat model that systemic administration of EP224283 diminishes ISR by reducing the PDGF-proliferation pathway of VSMC and the thrombogenicity. Local administration of this bioactive molecule carried by the stent may be promising in the treating ISR in high-risk population without increasing circulating drug levels (the potential side effects) as is the case for systemic administration.

Therefore, the anti-FXa activity assay (clinical routine method to monitor the activity of idraparinux or low molecular weight heparin) was performed to evaluate the antithrombotic activity of idraparinux [37] moieties of grafted EP224283-CoCr platform. As shown in Figure

10a, free solution of EP224283 at 2mg/ml exhibits an effective antithrombotic activity (2.21±0.08IU/ml). Even bare CoCr discs with physical adsorption of EP224283 showed certain anti-FXa activity (0.36±0.08IU/ml) compared with the substrate TCPS without EP224283 (0IU/ml). As expected, these results thus confirmed the potent antithrombotic activity of the EP224283 molecule.

When comparing the two different strategies of CoCr functionalisation (PDA-PEI-avidin and PDA-PEI-biotin-avidin) to graft EP224283, the PDA-PEI-avidin strategy exhibited a higher and significant anti-FXa activity (2.15±0.37 IU/ml), compared to the PDA-PEI-biotin-avidin strategy (1.46±0.23IU/ml). These results suggest that EP224283 was effectively grafted onto CoCr samples and preserved its bioactivity.

The major risk following stent implantation is in-stent restenosis and thrombosis. The latter occurs quickly following the implantation of a stent. It is therefore crucial to validate the anticoagulant activity of the molecule after immobilisation on the stent during the first week after implantation.

A degradation study in PBS was further carried out to determine the stability of grafted EP224283 from two functionalising strategies. Anti-FXa activity was thus used as an indicator to monitor the presence of EP224283 on the discs after different intervals of degradation. As shown in Figure 10b, the functionalisation of CoCr platforms with PDA-PEI-biotin +/- avidin offers longer anti-FXa activity of the surface of up to 7 days.

These degradation results evidenced the efficacy of the two functionalisation strategies proposed in this work. It was noted that the simple physical adsorption method (CoCr-EP224283) could only offer short-term anti-FXa activity at very low level that disappears overnight. Between the two strategies exposed, the PDA-PEI-avidin platform seems to be more efficient than the PDA-PEI-biotin-avidin one in terms of anti-FXa activity; the anti-FXa

activity of PDA-PEI-avidin-EP224283 exhibited a higher level at each time point, compared to the PDA-PEI-biotin-avidin-EP224283 functionalised platform.

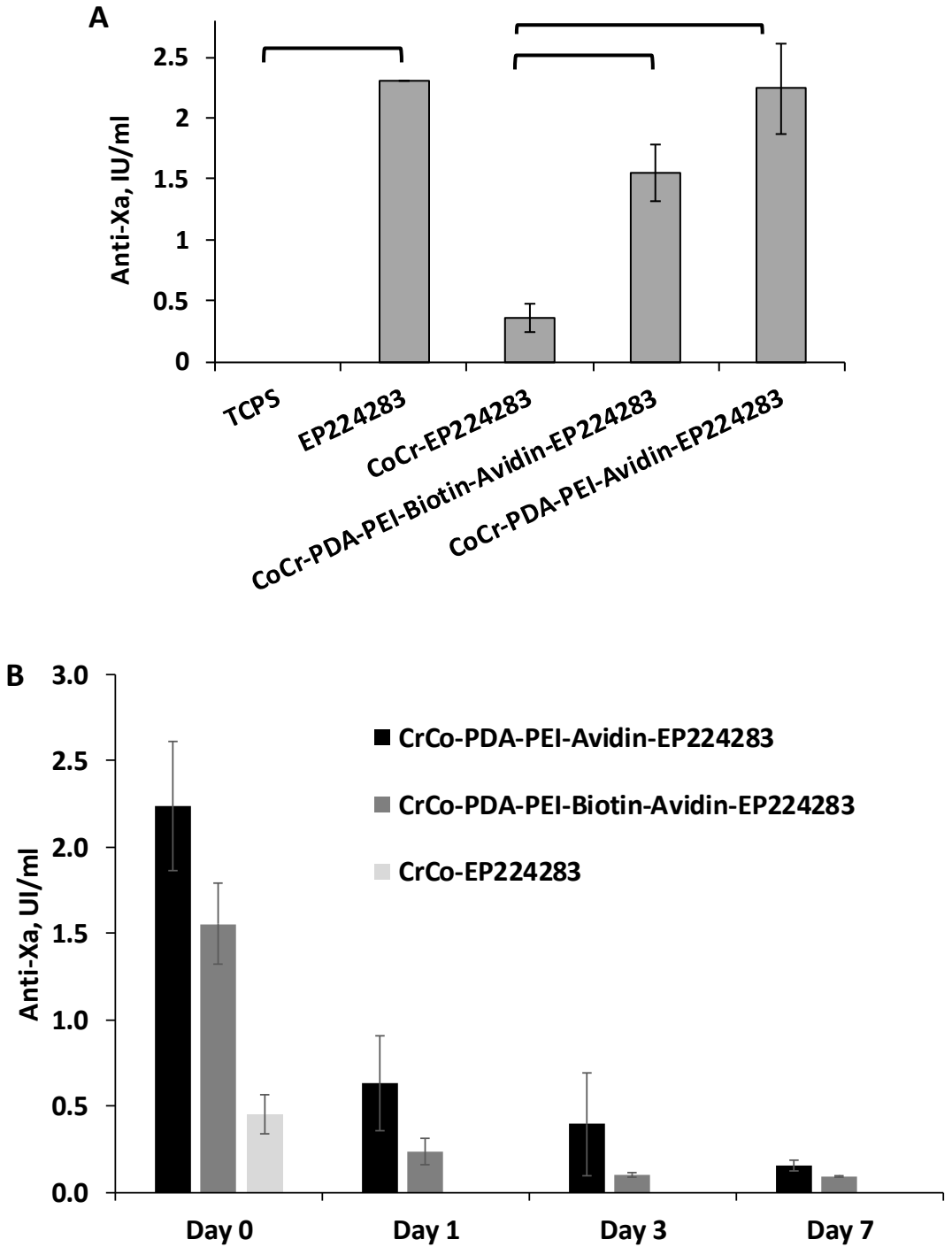

Figure 10: *In vitro* evaluation of anticoagulant activity (Anti-Xa factor) of EP224283 on bare and functionalised CoCr sample in comparison to TCPS and free molecule at T0 (A) and at different time of degradation in PBS (pH 7.4, 37°C, 80rpm) (B)

3.7 Platelet adhesion assay

In our previous study [15], systemic administration of idraparinux alone (anti-FXa activity) in a rat model failed to reduce restenosis. This implies that the activity of the tirofiban group of the molecule EP224283 has an important role for the success in reducing ISR [15,37]. Therefore, the inhibition of platelet activation by grafted EP224283 on the functionalised samples was evaluated through the platelet adhesion test, which is a first and essential step in the development of a thrombus [38,39].

Quantitative study of platelet adhesion by the LDH assay did not show any significant differences between the groups modified with the molecule EP224283 compared to control groups (data not shown) after 45 minutes of adhesion. Indeed, the tirofiban moiety of the molecule EP224283 is known for targeting the GPIIbIIIa (intergrin αIIbβ3) and inhibiting the platelet adhesion. This seems to be demonstrated by observing the shape of the adhered platelets by SEM. While tirofiban or other integrin antagonists are also found to cause "ligand-induced conformational changes" and result in ligand-induced integrin activation [40–43]. Although certain studies show that these monomeric RGD-like peptides (tirofiban) or compounds generally do not appear to directly induce integrin outside-in signaling [40–44], the adverse effect (thrombocytopenia, etc.) associated with the conformational changes induced by ligand mimetic antagonists should be carefully investigated.

Further examinations with thrombosis models in perfusion chambers [45,46] including testing its effect on blood coagulation in the flow [47], may be able to confirm its therapeutic potential.

Qualitative SEM analysis of platelet adhesion on bare or functionalised CoCr samples was shown in Figure 11. The morphology of the attached platelets on the bare CoCr surface after

30min of incubation (Figure 11a) was mostly fully spread with no distinct pseudopodia, corresponding to the highest degree of activation according to Goodman et al. [48], which is typical for the surface-induced platelet activation. To demonstrate the intrinsic anti-platelet activity of the molecule, a drop of EP224283 solution (2 mg/mL) was placed on the surface of bare CoCr, and with the evaporation of the liquid, EP224283 will stick on surfaces. The platelets on this CoCr-E224283 sample (Figure 11b) showed a dendritic form with early pseudopodia without flattening, which is in just the very early stage of activation and confirmed the anti-platelet activity of EP224283 (tirofiban moiety). Regarding two EP224293 immobilised groups, CoCr-PDA-PEI-biotin-avidin (Figure 11c) and CoCr-PDA-PEI-avidin (Figure 11d), the platelets presented a dendritic form similar to that on CoCr-E224283, which proves that the immobilised EP224283 on functionalised discs is still efficient in reducing activation of the platelet.

The key role of platelets in the ISR mechanisms was highlighted by basic and clinical studies. The relationship between early platelet mediated thrombus formation and late neointima development has also been well evidenced [49]. The positive effects of anti-platelet therapy after stent implantation are well known in current medical practice. However, the adverse effects of intensive anti-platelet therapy can expose patients to higher haemorrhage risk. A reduction of platelet activation by immobilised EP224283 on the functionalised CoCr surface sheds light on the efficacy of its local application and would help to alleviate the oral dual anti-platelet therapy currently required.

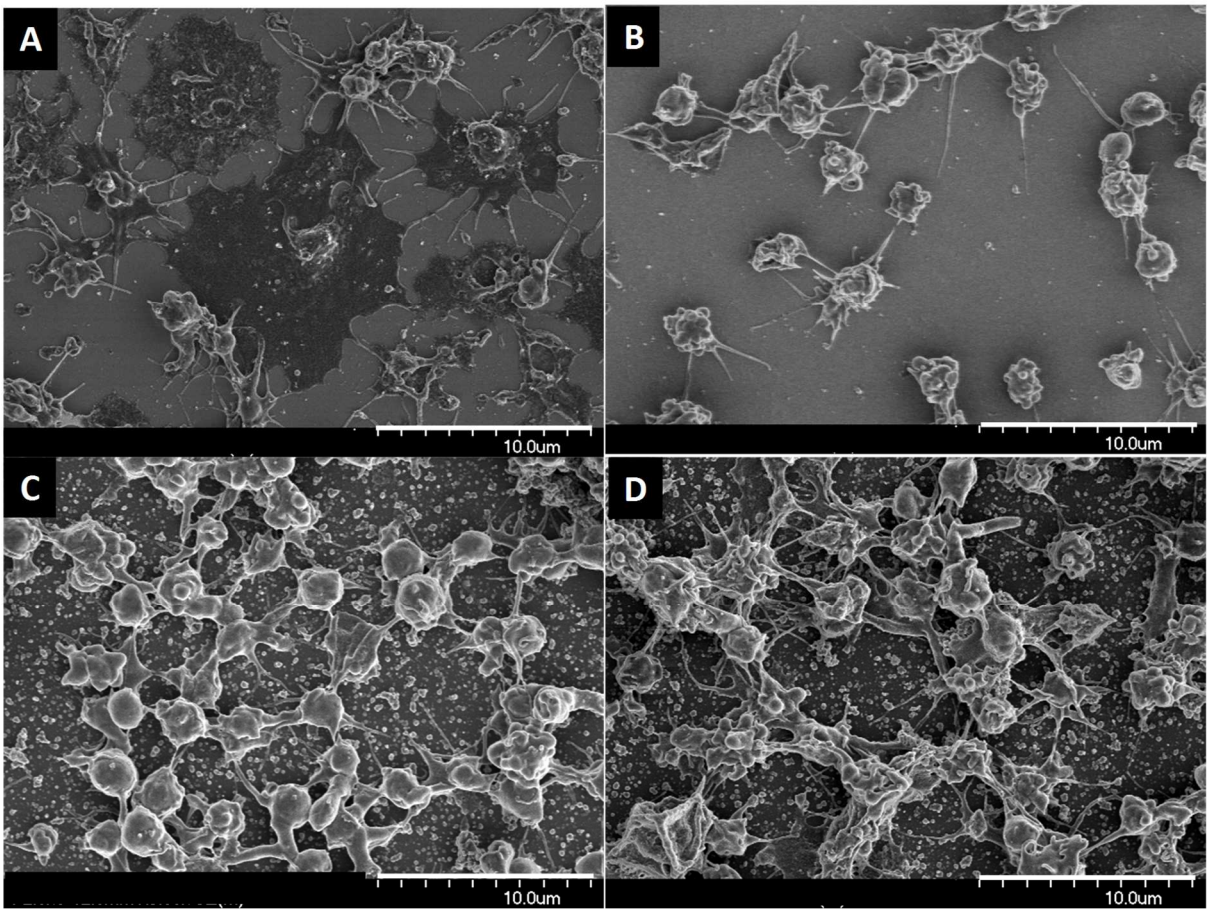

Figure 11: SEM images of platelets morphology on CoCr surface before (A) and after (B) deposition of EP224283, and on CrCo-PDA-PEI-biotin-avidin (C) and CrCo-PDA-PEI-avidin after grafting of EP224283 (D).

4 Conclusion

In this work, two strategies of functionalisation of a CoCr vascular stent with a bioinspired adhesive polymer (PDA) enriched in amine functions were reported for the immobilisation of an original anti-platelet and anti-thrombotic molecule (EP224283) with the objective of reducing acute thrombosis and ISR after stent implantation. The first strategy involves the biotinylation of the amine-rich PDA layer for the subsequent immobiliation of EP224283 onto the CoCr surface through biotin-avidin interactions while the second strategy consists of the direct immobilisation of avidin onto the amine-rich PDA layer via coupling reactions. Both strategies allowed the fixation of the EP224283 molecule onto the CoCr stent, which

maintains its therapeutic properties. Interestingly, the strategy employing the direct immobilisation of avidin onto the stent surface (CoCr-PDA-PEI-avidin) offers the possibility of extending the therapeutic activity of the EP224283 molecule for up to seven days.

As anticipated, this new stent functionalised with the EP224283 agent would alleviate the need for a long and aggressive oral dual anti-platelet/anti-thrombotic therapy period after implantation. Moreover, the combination of anti-platelet aggregation and anti-coagulant effect on the stent surface could limit ISR.

Acknowledgments: The authors would like to thank the French Society of Radiology (SFR), and FRI for financial support, Abbott Vascular and Endotis for provided stents and molecules, Dr. Ahmed Addad from UMET for carrying out SEM images and related discussions and Mr Mickael Maton from U1008 for his help on stent functionalisation.

Conflict Of Interest

Authors have no conflict of interest

REFERENCES

[1] D.L. Fischman, M.B. Leon, D.S. Baim, R.A. Schatz, M.P. Savage, I. Penn, K. Detre, L. Veltri, D. Ricci, M. Nobuyoshi, A randomized comparison of coronary-stent placement and balloon angioplasty in the treatment of coronary artery disease. Stent Restenosis Study Investigators, N. Engl. J. Med. 331 (1994) 496–501. https://doi.org/10.1056/NEJM199408253310802.

[2] J.W. Moses, M.B. Leon, J.J. Popma, P.J. Fitzgerald, D.R. Holmes, C. O'Shaughnessy, R.P. Caputo, D.J. Kereiakes, D.O. Williams, P.S. Teirstein, J.L. Jaeger, R.E. Kuntz, SIRIUS Investigators, Sirolimus-eluting stents versus standard stents in patients with stenosis in a native coronary artery, N. Engl. J. Med. 349 (2003) 1315–1323. https://doi.org/10.1056/NEJMoa035071.

[3] A. Lejay, Y. Georg, C. Bajcz, F. Thaveau, B. Geny, J.-G. Kretz, N. Chakfé, Endovascular treatment of infra-popliteal arteries in patients with critical limb ischemia, Acta Chir. Belg. 109 (2009) 684–693.

[4] A. Gaspardone, F. Versaci, Coronary Stenting and Inflammation, Am. J. Cardiol. 96 (2005) 65–70. https://doi.org/10.1016/j.amjcard.2005.09.064.

[5] A. Muto, T.N. Fitzgerald, J.M. Pimiento, S.P. Maloney, D. Teso, J.J. Paszkowiak, T.S. Westvik, F.A. Kudo, T. Nishibe, A. Dardik, Smooth muscle cell signal transduction: Implications of vascular biology for vascular surgeons, J. Vasc. Surg. 45 (2007) A15–A24. https://doi.org/10.1016/j.jvs.2007.02.061.

[6] A. Curcio, D. Torella, C. Indolfi, Mechanisms of smooth muscle cell proliferation and endothelial regeneration after vascular injury and stenting: approach to therapy, Circ. J. Off. J. Jpn. Circ. Soc. 75 (2011) 1287–1296.

[7] J. Hallas, M. Dall, A. Andries, B.S. Andersen, C. Aalykke, J.M. Hansen, M. Andersen, A.T. Lassen, Use of single and combined antithrombotic therapy and risk of serious upper gastrointestinal bleeding: population based case-control study, BMJ. 333 (2006) 726. https://doi.org/10.1136/bmj.38947.697558.AE.

[8] H. Lee, S.M. Dellatore, W.M. Miller, P.B. Messersmith, Mussel-inspired surface chemistry for multifunctional coatings, Science. 318 (2007) 426–430. https://doi.org/10.1126/science.1147241.

[9] Z. Yang, Q. Tu, Y. Zhu, R. Luo, X. Li, Y. Xie, M.F. Maitz, J. Wang, N. Huang, Mussel-Inspired Coating of Polydopamine Directs Endothelial and Smooth Muscle Cell Fate for Re-endothelialization of Vascular Devices, Adv. Healthc. Mater. 1 (2012) 548–559. https://doi.org/10.1002/adhm.201200073.

[10] J. Sobocinski, W. Laure, M. Taha, E. Courcot, F. Chai, N. Simon, A. Addad, B. Martel, S. Haulon, P. Woisel, N. Blanchemain, J. Lyskawa, Mussel inspired coating of a biocompatible cyclodextrin based polymer onto CoCr vascular stents, ACS Appl. Mater. Interfaces. 6 (2014) 3575–3586. https://doi.org/10.1021/am405774v.

[11] Y. Weng, Q. Song, Y. Zhou, L. Zhang, J. Wang, J. Chen, Y. Leng, S. Li, N. Huang, Immobilization of selenocystamine on TiO2 surfaces for in situ catalytic generation of nitric oxide and potential application in intravascular stents, Biomaterials. 32 (2011) 1253–1263. https://doi.org/10.1016/j.biomaterials.2010.10.039.

[12] Y. Yang, P. Qi, F. Wen, X. Li, Q. Xia, M.F. Maitz, Z. Yang, R. Shen, Q. Tu, N. Huang, Mussel-inspired one-step adherent coating rich in amine groups for covalent immobilization of heparin: hemocompatibility, growth behaviors of vascular cells, and tissue response, ACS Appl. Mater. Interfaces. 6 (2014) 14608–14620. https://doi.org/10.1021/am503925r.

[13] D. Zheng, K.G. Neoh, Z. Shi, E.-T. Kang, Assessment of stability of surface anchors for antibacterial coatings and immobilized growth factors on titanium, J. Colloid Interface Sci. 406 (2013) 238–246. https://doi.org/10.1016/j.jcis.2013.05.060.

[14] B. Hechler, M. Freund, G. Alame, C. Leguay, S. Gaertner, J.-P. Cazenave, M. Petitou, C. Gachet, The Antithrombotic Activity of EP224283, a Neutralizable Dual Factor Xa Inhibitor/Glycoprotein IIbIIIa Antagonist, Exceeds That of the Coadministered Parent Compounds, J. Pharmacol. Exp. Ther. 338 (2011) 412–420. https://doi.org/10.1124/jpet.111.181321.

[15] B. Maurel, F. Chai, M. Maton, N. Blanchemain, S. Haulon, In stent restenosis and thrombosis assessment after EP224283 injection in a rat model, Atherosclerosis. 229 (2013) 462–468. https://doi.org/10.1016/j.atherosclerosis.2013.06.009.

[16] C. Boyer, J. Liu, V. Bulmus, T.P. Davis, C. Barner-Kowollik, M.H. Stenzel, Direct Synthesis of Well-Defined Heterotelechelic Polymers for Bioconjugations, Macromolecules. 41 (2008) 5641–5650. https://doi.org/10.1021/ma800289u.

[17] X. Jiang, M. Ahmed, Z. Deng, R. Narain, Biotinylated Glyco-Functionalized Quantum Dots: Synthesis, Characterization, and Cytotoxicity Studies, Bioconjug. Chem. 20 (2009) 994–1001. https://doi.org/10.1021/bc800566f.

[18] X. Huang, C. Boyer, T.P. Davis, V. Bulmus, Synthesis of heterotelechelic polymers with affinity to glutathione-S-transferase and biotin-tagged proteins by RAFT polymerization and thiol–ene reactions, Polym. Chem. 2 (2011) 1505. https://doi.org/10.1039/c1py00049g.

[19] C.-M. Pradier, M. Salmain, L. Zheng, G. Jaouen, Specific binding of avidin to biotin immobilised on modified gold surfaces: Fourier transform infrared reflection absorption spectroscopy analysis, Surf. Sci. 502 (2002) 193–202.

[20] A. Pérez-Anes, M. Gargouri, W. Laure, H. Van Den Berghe, E. Courcot, J. Sobocinski, N. Tabary, F. Chai, J.-F. Blach, A. Addad, P. Woisel, D. Douroumis, B. Martel, N. Blanchemain, J. Lyskawa, Bioinspired Titanium Drug Eluting Platforms Based on a Poly-β-cyclodextrin–Chitosan Layer-by-Layer Self-Assembly Targeting Infections, ACS Appl. Mater. Interfaces. (2015) 150603102511002. https://doi.org/10.1021/acsami.5b02402.

[21] G. Mayer, N. Blanchemain, C. Dupas-Bruzek, V. Miri, M. Traisnel, L. Gengembre, D. Derozier, H.F. Hildebrand, Physico-chemical and biological evaluation of excimer laser irradiated polyethylene terephthalate (pet) surfaces, Biomaterials. 27 (2006) 553–566. https://doi.org/10.1016/j.biomaterials.2005.05.096.

[22] E. Kurin, A.G. Atanasov, O. Donath, E.H. Heiss, V.M. Dirsch, M. Nagy, Synergy study of the inhibitory potential of red wine polyphenols on vascular smooth muscle cell

proliferation, Planta Med. 78 (2012) 772–778. https://doi.org/10.1055/s-0031-1298440.

[23] Y. Liu, R. Luo, F. Shen, L. Tang, J. Wang, N. Huang, Construction of mussel-inspired coating via the direct reaction of catechol and polyethyleneimine for efficient heparin immobilization, Appl. Surf. Sci. 328 (2015) 163–169. https://doi.org/10.1016/j.apsusc.2014.12.004.

[24] P. Vermette, T. Gengenbach, U. Divisekera, P.A. Kambouris, H.J. Griesser, L. Meagher, Immobilization and surface characterization of NeutrAvidin biotin-binding protein on different hydrogel interlayers, J. Colloid Interface Sci. 259 (2003) 13–26. https://doi.org/10.1016/S0021-9797(02)00185-6.

[25] M.I. Castellanos, C. Mas-Moruno, A. Grau, X. Serra-Picamal, X. Trepat, F. Albericio, M. Joner, F.J. Gil, M.P. Ginebra, J.M. Manero, M. Pegueroles, Functionalization of CoCr surfaces with cell adhesive peptides to promote HUVECs adhesion and proliferation, Appl. Surf. Sci. 393 (2017) 82–92. https://doi.org/10.1016/j.apsusc.2016.09.107.

[26] Z. Chen, Q. Li, J. Chen, R. Luo, M.F. Maitz, N. Huang, Immobilization of serum albumin and peptide aptamer for EPC on polydopamine coated titanium surface for enhanced in-situ self-endothelialization, Mater. Sci. Eng. C. 60 (2016) 219–229. https://doi.org/10.1016/j.msec.2015.11.044.

[27] K.-Y. Ju, Y. Lee, S. Lee, S.B. Park, J.-K. Lee, Bioinspired Polymerization of Dopamine to Generate Melanin-Like Nanoparticles Having an Excellent Free-Radical-Scavenging Property, Biomacromolecules. 12 (2011) 625–632. https://doi.org/10.1021/bm101281b.

[28] J.T. Arena, B. McCloskey, B.D. Freeman, J.R. McCutcheon, Surface modification of thin film composite membrane support layers with polydopamine: Enabling use of reverse

osmosis membranes in pressure retarded osmosis, J. Membr. Sci. 375 (2011) 55–62. https://doi.org/10.1016/j.memsci.2011.01.060.

[29] W. Zhe, C. Dong, Y. Sefei, Z. Dawei, X. Kui, L. Xiaogang, Facile incorporation of hydroxyapatite onto an anodized Ti surface via a mussel inspired polydopamine coating, Appl. Surf. Sci. 378 (2016) 496–503. https://doi.org/10.1016/j.apsusc.2016.03.094.

[30] X. Wang, S. Yuan, D. Shi, Y. Yang, T. Jiang, S. Yan, H. Shi, S. Luan, J. Yin, Integrated antifouling and bactericidal polymer membranes through bioinspired polydopamine/poly(N-vinyl pyrrolidone) coating, Appl. Surf. Sci. 375 (2016) 9–18. https://doi.org/10.1016/j.apsusc.2016.01.198.

[31] W. Shen, K. Cai, Z. Yang, Y. Yan, W. Yang, P. Liu, Improved endothelialization of NiTi alloy by VEGF functionalized nanocoating, Colloids Surf. B Biointerfaces. 94 (2012) 347–353. https://doi.org/10.1016/j.colsurfb.2012.02.009.

[32] Y. Feng, X. Ma, L. Chang, S. Zhu, S. Guan, Characterization and cytocompatibility of polydopamine on MAO-HA coating supported on Mg-Zn-Ca alloy, Surf. Interface Anal. 49 (2017) 1115–1123. https://doi.org/10.1002/sia.6286.

[33] Y.H. Ding, M. Floren, W. Tan, Mussel-inspired polydopamine for bio-surface functionalization, Biosurface Biotribology. 2 (2016) 121–136. https://doi.org/10.1016/j.bsbt.2016.11.001.

[34] X. Li, J. Deng, S. Yuan, J. Wang, R. Luo, S. Chen, J. Wang, N. Huang, Fabrication of endothelial progenitor cell capture surface via DNA aptamer modifying dopamine/polyethyleneimine copolymer film, Appl. Surf. Sci. 386 (2016) 138–150. https://doi.org/10.1016/j.apsusc.2016.06.015.

[35] D.G. Graham, S.M. Tiffany, W.R. Bell, W.F. Gutknecht, Autoxidation versus covalent

binding of quinones as the mechanism of toxicity of dopamine, 6-hydroxydopamine, and related compounds toward C1300 neuroblastoma cells in vitro, Mol. Pharmacol. 14 (1978) 644–653.

[36] Y. Ding, L.-T. Weng, M. Yang, Z. Yang, X. Lu, N. Huang, Y. Leng, Insights into the Aggregation/Deposition and Structure of a Polydopamine Film, Langmuir. 30 (2014) 12258–12269. https://doi.org/10.1021/la5026608.

[37] X.R. Xu, N. Carrim, M.A.D. Neves, T. McKeown, T.W. Stratton, R.M.P. Coelho, X. Lei, P. Chen, J. Xu, X. Dai, B.X. Li, H. Ni, Platelets and platelet adhesion molecules: novel mechanisms of thrombosis and anti-thrombotic therapies, Thromb. J. 14 (2016) 29. https://doi.org/10.1186/s12959-016-0100-6.

[38] S.P. Jackson, The growing complexity of platelet aggregation, Blood. 109 (2007) 5087–5095. https://doi.org/10.1182/blood-2006-12-027698.

[39] Y. Wang, R.C. Gallant, H. Ni, Extracellular matrix proteins in the regulation of thrombus formation, Curr. Opin. Hematol. 23 (2016) 280–287. https://doi.org/10.1097/MOH.0000000000000237.

[40] D. Cox, R. Smith, M. Quinn, P. Theroux, P. Crean, D.J. Fitzgerald, Evidence of platelet activation during treatment with a GPIIb/IIIa antagonist in patients presenting with acute coronary syndromes, J. Am. Coll. Cardiol. 36 (2000) 1514–1519. https://doi.org/10.1016/s0735-1097(00)00919-0.

[41] B. Estevez, B. Shen, X. Du, Targeting Integrin and Integrin Signaling in Treating Thrombosis, Arterioscler. Thromb. Vasc. Biol. 35 (2015) 24–29. https://doi.org/10.1161/ATVBAHA.114.303411.

[42] R.R. Hantgan, M.C. Stahle, Integrin priming dynamics: mechanisms of integrin

antagonist-promoted alphaIIbbeta3:PAC-1 molecular recognition, Biochemistry. 48 (2009) 8355–8365. https://doi.org/10.1021/bi900475k.

[43] L.K. Jennings, J.H. Haga, S.M. Slack, Differential expression of a ligand induced binding site (LIBS) by GPIIb-IIIa ligand recognition peptides and parenteral antagonists, Thromb. Haemost. 84 (2000) 1095–1102.

[44] N. Bassler, C. Loeffler, P. Mangin, Y. Yuan, M. Schwarz, C.E. Hagemeyer, S.U. Eisenhardt, I. Ahrens, C. Bode, S.P. Jackson, K. Peter, A mechanistic model for paradoxical platelet activation by ligand-mimetic alphaIIb beta3 (GPIIb/IIIa) antagonists, Arterioscler. Thromb. Vasc. Biol. 27 (2007) e9-15. https://doi.org/10.1161/01.ATV.0000255307.65939.59.

[45] X.R. Xu, Y. Wang, R. Adili, L. Ju, C.M. Spring, J.W. Jin, H. Yang, M.A.D. Neves, P. Chen, Y. Yang, X. Lei, Y. Chen, R.C. Gallant, M. Xu, H. Zhang, J. Song, P. Ke, D. Zhang, N. Carrim, S.-Y. Yu, G. Zhu, Y.-M. She, T. Cyr, W. Fu, G. Liu, P.W. Connelly, M.L. Rand, K. Adeli, J. Freedman, J.E. Lee, P. Tso, P. Marchese, W.S. Davidson, S.P. Jackson, C. Zhu, Z.M. Ruggeri, H. Ni, Apolipoprotein A-IV binds αIIbβ3 integrin and inhibits thrombosis, Nat. Commun. 9 (2018) 3608. https://doi.org/10.1038/s41467-018-05806-0.

[46] G. Zhu, Q. Zhang, E.C. Reddy, N. Carrim, Y. Chen, X.R. Xu, M. Xu, Y. Wang, Y. Hou, L. Ma, Y. Li, M. Rui, T.N. Petruzziello-Pellegrini, C. Lavalle, T.W. Stratton, X. Lei, R. Adili, P. Chen, C. Zhu, J.A. Wilkins, R.O. Hynes, J. Freedman, H. Ni, The integrin PSI domain has an endogenous thiol isomerase function and is a novel target for antiplatelet therapy, Blood. 129 (2017) 1840–1854. https://doi.org/10.1182/blood-2016-07-729400.

[47] C. Li, S. Piran, P. Chen, S. Lang, A. Zarpellon, J.W. Jin, G. Zhu, A. Reheman, D.E. van der Wal, E.K. Simpson, R. Ni, P.L. Gross, J. Ware, Z.M. Ruggeri, J. Freedman, H. Ni, The maternal immune response to fetal platelet GPIbα causes frequent miscarriage in mice that can be prevented by intravenous IgG and anti-FcRn therapies, J. Clin. Invest. 121 (2011)

4537–4547. https://doi.org/10.1172/JCI57850.

[48] S.L. Goodman, R.M. Albrecht, Correlative light and electron microscopy of platelet adhesion and fibrinogen receptor expression using colloidal-gold labeling, Scanning Microsc. 1 (1987) 727–734.

[49] D.J.W. Evans, L.E. Jackman, J. Chamberlain, D.J. Crosdale, H.M. Judge, K. Jetha, K.E. Norman, S.E. Francis, R.F. Storey, Platelet P2Y $_{12}$ Receptor Influences the Vessel Wall Response to Arterial Injury and Thrombosis, Circulation. 119 (2009) 116–122. https://doi.org/10.1161/CIRCULATIONAHA.107.762690.